Applied Physics A (2020) 126:891
https://doi.org/10.1007/s00339-020-03955-y

Applied Physics A
Materials Science & Processing

Deposition geometry effect on structural, morphological and optical properties of Nb_2O_5 nanostructure prepared by hydrothermal technique

Evan T. Salim[1] · Raid A. Ismail[1] · Halemah T. Halbos[1]

Received: 26 November 2019 / Accepted: 29 August 2020 / Published online: 26 October 2020

Abstract

This work aims to explain the effect of substrate position and deposition angle on the structural, optical, and morphological properties of niobium pentoxide (Nb_2O_5) thin films prepared by hydrothermal technique. Three different surface morphologies, namely flake-, rod-, and spring-like nanostructures, were obtained using three sample holders with different geometries. X-ray diffraction results confirm the formation of polycrystalline rod-like Nb_2O_5 highly oriented in the direction of (-402) plane. The direct optical energy gaps at the different deposition geometries varied from 2.9 to 3.4 eV.

Keywords Surface morphologies · Substrate position · Deposition angle · Optical properties · Nb_2O_5 thin films

1 Introduction

Niobium oxides can exhibit different properties, which make them a versatile material [1–3]. Nb_2O_5 films have remarkable optical and structural properties such as high refractive index, low optical absorption in the visible and near-infrared regions, corrosion resistance, superior thermal stability, and excellent chemical stability [4–6]. Their physical properties (optical, electrical, and structural properties) strongly depend on their stoichiometry, crystal structure, and surface roughness [7–10]. Nb_2O_5 can be synthesized using several techniques, such as hydrothermal [11, 12], anodization [13, 14], electrodeposition [15, 16], sol–gel spin-coating [17, 18], sputtering [19, 20], and pulsed laser deposition [21, 22]. In particular, the hydrothermal method is a simple, cost-effective, and low-temperature process of growing single-crystalline oxide nanostructures [23–28]. Nb_2O_5 nanostructures exhibit various morphologies, such as nanowires, nanobelts, nanorods, nanotubes, opal nanostructure, mesoporous, and hollow nanospheres [5, 29–39]. However, the hydrothermal-based Nb_2O_5 nanostructure is not extensively investigated, and its structure variations are also limited [40]. In addition, the hydrothermal method is the most popular preparation technique for nanohybrid materials and nanocomposites. Hydrothermal expression has originated from simple geological ancestry and was first used by Sir Roderick Murchison [41] to explain the effect of high temperature, water, and pressure on the earth's crust and on the formation of different minerals and rocks. The hydrothermal method is also defined as a chemical reaction that occurs in different solvents at elevated temperatures and pressure above 1 atm in a closed autoclave [41, 42]. In nanotechnology field, this technique has an advantage over others, because it is ideal for preparing specifically design molecules, i.e., high quality, high purity, and improved crystalline, with desirable chemical and physical properties and great industrial application [43].

In this process, dissolved metal ions are heated at a constant temperature for a specific time. For Nb_2O_5 preparation, the Nb^{5+} ion solution is obtained either through the action of the mineral acid of niobium metal or the dissolution of niobium salt-like $NbCl_5$ [34, 35]. This method involves several steps such as nucleation and growth of naturally crystalline Nb_2O_5 under specific temperature and pressure to allow the relatively insoluble crystalline materials to dissolve under ordinary conditions. Good control of the preparation conditions is an advantage of hydrothermal method over the pyrochemical method. Adjusting the temperature, time, pressure, caustic soda concentration, solid–liquid ratio, and additives

✉ Evan T. Salim
evan_tarq@yahoo.com; 100354@uotechnology.edu.iq

[1] Applied Science Department, University of Technology, Baghdad 10066, Iraq

may control the properties, particle size, and morphology of the products [38].

Different nanostructure materials have been prepared under various conditions using hydrothermal method. For example, Bai et al. deposited CdS nanofilms on Al_2O_3 substrates using hydrothermal method and obtained a hexagonal morphology with improved optical properties [44, 45]. ZnO nanofilms with macroporous morphology were prepared using the same process for electrochemical hydrogen storage and possible industrial production [46, 47]. Volanti et al. used the hydrothermal method in a microwave oven to prepare CuO nanoflower and employed FE–SEM and TEM to estimate the diameter of the sphere and monitor the thorn of the flower-nanostructures, respectively [48]. Bavykin et al. studied the effect of hydrothermal preparation on TiO_2 nanotube morphology by preparing the nonmaterial at low temperature and examining nitrogen absorption during the process. Their results revealed that the diameter of the average nanotube depends on temperature and TiO_2 weight in the sodium hydroxide solution [49]. Wang et al. prepared lead chalcogenides through the hydrothermal reaction of lead acetate with tellurium and selenium in sodium hydroxide solution and found that different nanocrystals morphologies could be obtained under specific conditions [50]. Skrodczky et al. found a strong relationship between the type of strong acid sites and the specifically obtained Nb_2O_5 nanostructure and presented a synthesis approach for Nb_2O_5 nanostructures that have different structures and can be used as efficient catalysts [51].

An additional essential factor that affects surface morphology and film properties is the use of an oblique angle during deposition to obtain highly porous thin films [52, 53]. In the last 20 years, oblique deposition has been used in manufacturing many devices for magnetism, photovoltaic, sensors, and optical application [54, 55].

To the best of our knowledge, the combination of hydrothermal and oblique deposition has never been applied to obtain different structures and morphologies for various applications in the future.

Therefore, the present study focused on the effect of deposition angle on the characteristics of nanostructured Nb_2O_5 film to improve its growth quality using hydrothermal method. Nb_2O_5thin films were synthesized via hydrothermal method.

2 Experimental

In brief, 0.1 g of commercial metal Nb powder was dispersed into 40 mL of distilled water and stirred for 30 min. The prepared solution was transferred into a sealed Teflon-lined stainless steel autoclave of 50 mL capacity. Hydrothermal growth was facilitated at 160 °C for 72 h. The following three different geometries were used to deposit the film: the quartz substrates were immersed in the precursor solutions in the positions of flat at 0° angle, 45° with zero height, and 45° with 3 cm height as shown in Fig. 1. After the reaction, the autoclave was cooled down naturally to room temperature. UV–vis spectrophotometer (model T60) and X-ray diffractometer (Shimadzu 6000) were employed to determine the optical and structural properties of the deposited films, respectively. Scanning electron microscope (AA-3000) type was used to examine the morphological and grain size of the films.

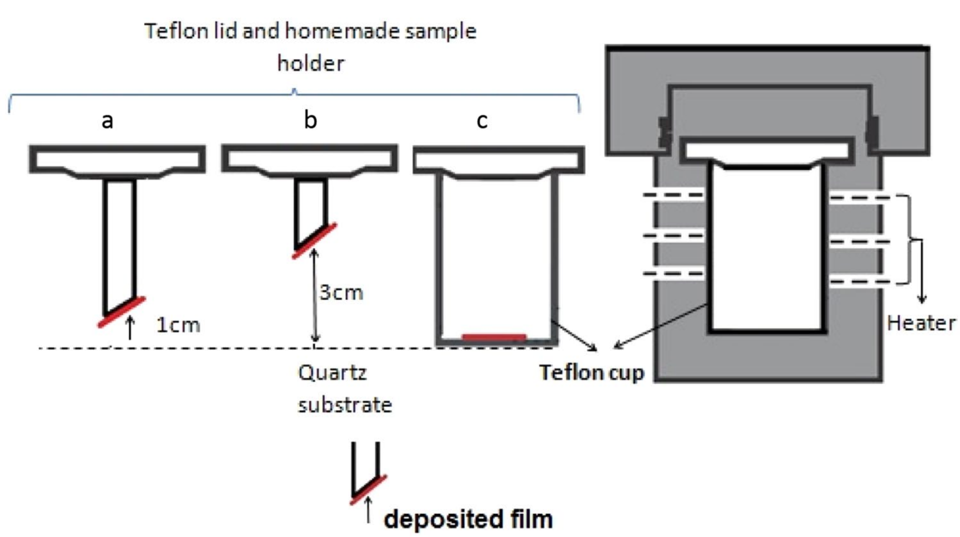

Fig. 1 schematic diagram of the substrate holder used inside the sealed Teflon-lined autoclave

3 Results and discussion

The XRD patterns of the Nb_2O_5 thin film are shown in Fig. 2a–c. The prepared samples were hydrothermally synthesized, and the substrate was placed at three different positions inside the sealed Teflon-lined autoclave. The crystal structure in Fig. 2a represents the first position of the Nb_2O_5 thin film when the substrate was placed at an oblique angle. Peak spectra confirmed the polycrystalline nature of the nanostructures. The results displayed three intense peaks related to the formation of Nb_2O_5 nanostructure. One strong peak indicates the high crystalline nature of the sample, thus coinciding with the X-ray diffraction peaks of the standard card (00-030-0872) of Nb_2O_5 at $2\theta = 38.3°$ related to the diffraction planes at (-402). The other two diffraction peak coincided with the standard card (00-030-0872) of Nb_2O_5 at $2\theta = (46.0°$ and $55.3°)$ related to the diffraction planes (002) and (202) belonging to Nb_2O_5 thin films. The existence of non-oxidized Nb (JCPDS 00-034-0370) was confirmed by the diffraction peak at 69.6°. In this work, Nb and H_2O_2 were used as the mineralizing agent and oxidant in the hydrothermal environment. The following chemical reactions are expected to occur during the hydrothermal process [56]:

$$2Nb + 5H_2O_2Nb_2O_5 + 5H_2O. \tag{1}$$

At the beginning of the hydrothermal reaction, Nb ions are released and then indirectly oxidized by H_2O_2. Figure 1b illustrates the second position of the Nb_2O_5 thin film when the substrate was placed at 0° angle. All positions of the diffraction peaks had reduced intensity, which is similar to those of the sample in the first position. This finding may be related to the inner stress that was expected to occur when the metal Nb was converted into Nb_2O_5 in situ due to the different lattice parameters and the appearance of another diffraction peak at approximately 21.0° (100) belonging to the Nb metal. Figure 2c represents the third position of the Nb_2O_5 thin film at 45° with height of 3.6 cm inside the Teflon-lined autoclave. Two diffraction peaks belonging to $Nb_2O_5$and another Nb metal were observed. Although the purity of Nb_2O_5 thin film in the final product can still be improved, the proposed synthesis route is simple and does not require any templates or catalysts introduced into the reaction system. However, its reaction time is longer than

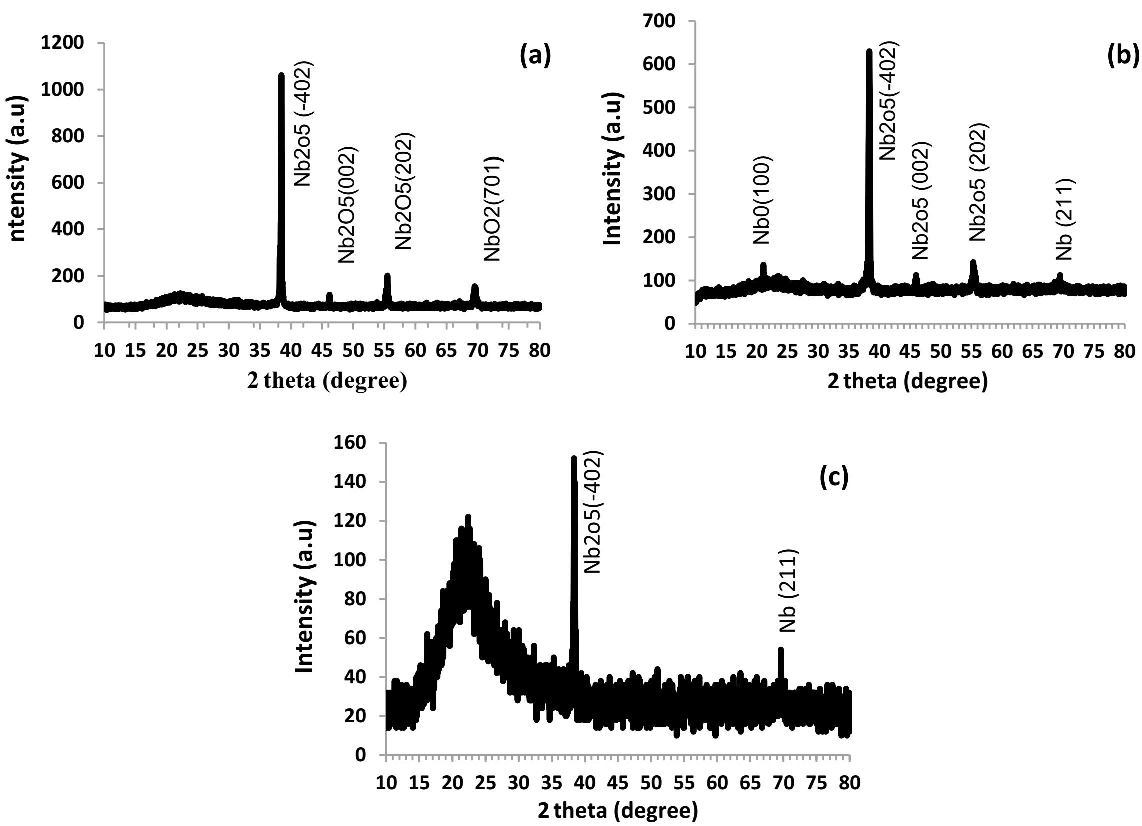

Fig. 2 XRD patterns of Nb_2O_5 thin films deposited at three different positions **a** substrate at 45° and 1 cm high, **b** substrate at angle 45° and 3 cm height and **c** substrate at 0° angle

that of the normal hydrothermal process. This phenomenon occurred, because the hydrothermal reaction is accelerated in the presence of templates or catalysts [57].

The estimated crystalline size, stress, and strain values at different deposition conditions and for the moderate diffraction plane (-402) are displayed in Table 1. The crystalline size slightly increased under the oblique deposition with different heights and significantly increased for the substrate holder at flat 0° angle. The slight increase may be related to the shadow effect at glancing angle deposition. The strain and stress values also show a comparable value for oblique deposition while a slight difference could be noticed for 0° angle deposition. The optical absorbance spectra within 300–900 nm wavelengths of Nb_2O_5 thin films for the three samples prepared on a quartz substrate at different angles in Teflon-lined autoclave are presented in Fig. 3. Different absorption values were obtained for the three prepared films. The maximum absorbance appear in the wavelength range of 300–380 nm for three sample prepared due to its wide energy gap. This finding has good agreement with [58–62]. The high absorption of the films shows many potential applications in the UV–vis range. The sharp band edge in the UV spectral region ensures the formation of direct bandgaps for all prepared thin films. Their values were obtained using the following mathematical expression [63]:

$$\alpha h\nu = A(h\nu - Eg)^{1/2}. \quad (2)$$

α is the absorption coefficient, hν is the incident photon energy, and A is the constant. The obtained energy gap values in Fig. 2 were approximately 2.9, 3.15, and 3.4 eV for the three samples prepared at different angles. These results indicate that the sample at oblique angle has lower energy band gap than the excited UV light source, making it a suitable candidate for UV sensor [64–67].

Surface engineering is one of the most important aspects that highly affect the scientific and industrial applications of any material. Technologies that require highly structured and porous films have reinforced the development of thin films with improved morphological properties. The influence of deposition angle and height on the surface morphology of Nb_2O_5 thin films was studied using SEM. Figure 4a–c shows different morphologies for the films with substrate deposited at different angles in Teflon-lined autoclave at 160 °C for 72 h. Nb_2O_5 highly uniform smooth and clear nanoflake-like nanostructure was formed (Fig. 4a) when the substrate was positioned at oblique angle of 45° with 1 cm height in an autoclave. At the same angle with different height of approximately 3.5 cm, a horizontally aligned rod-like nanostructure with completely different morphology was obtained and is shown in Fig. 4b. Numerous helical spring-like structures were obtained in the sample prepared using 0° angle holder as shown in Fig. 4c. These Nb_2O_5 nanorods appeared close to each other with a smooth surface. The structure is further highlighted in Fig. 4c with high magnification revealing a peculiar helical spring-like nanostructure. The Nb_2O_5 helical spring nanorods appeared as many layers that are adjacent to other. In the case of oblique deposition when the deposited particles arrived at a glancing angle to the substrate surface, additional factors affected the growth process and consequently the microstructure film properties. This factor is called "shadowing effect", which prevents particle deposition in the regions behind the first formed nuclei. Different morphologies could be obtained depending on this shadowing effect [54]. In the case of helical spring morphology obtained at 0° angle deposition, the substrate rotated around the azimuthally axis (ϕ), and the remaining zenithal angle (α) constant provided a single degree of freedom to control the film nanostructure. This phenomenon is sometimes referred to as "dynamic" oblique film deposition. In this way, singular shapes such as spirals or helixes could be obtained [68, 69]. The oblique deposition affects the area responsible for the surface shadowing of vapor species, thus explaining the different relations between the incident angle of the deposition flux and the tilt angle of the growing columns [70]. The stoichiometry of the prepared thin film was estimated according to the mass percentage of Nb and O extracted from EDS results as shown in Fig. 5a–c, and the values are shown in Table 2. The [Nb]/[O] mass ratio is a function of sample height and glazing angle. The mass ratio of the oblique samples with different heights was in the range of 2.04–5.92. An optimum percentage value was obtained for film deposited at 0°angles and reflected the stoichiometry of approximately 99%.

Table 1 Estimated crystalline size, stress and strain for (−402) diffraction plane at different deposition condition

Position angle	Peaks	*hkl*	B_{size}	Crystalline size D (nm)	$\delta \times 10^{-3}$ lines/m^2	Strain ε
45 and 1 cm height	38.34	−402	0.24	43.98	5.16	0.29
45 and height 3 cm	38.3	−402	0.22	44	5.1	0.28
Zero angle flat substrate holder	38.38	−402	0.20	48.2	4.2	0.26

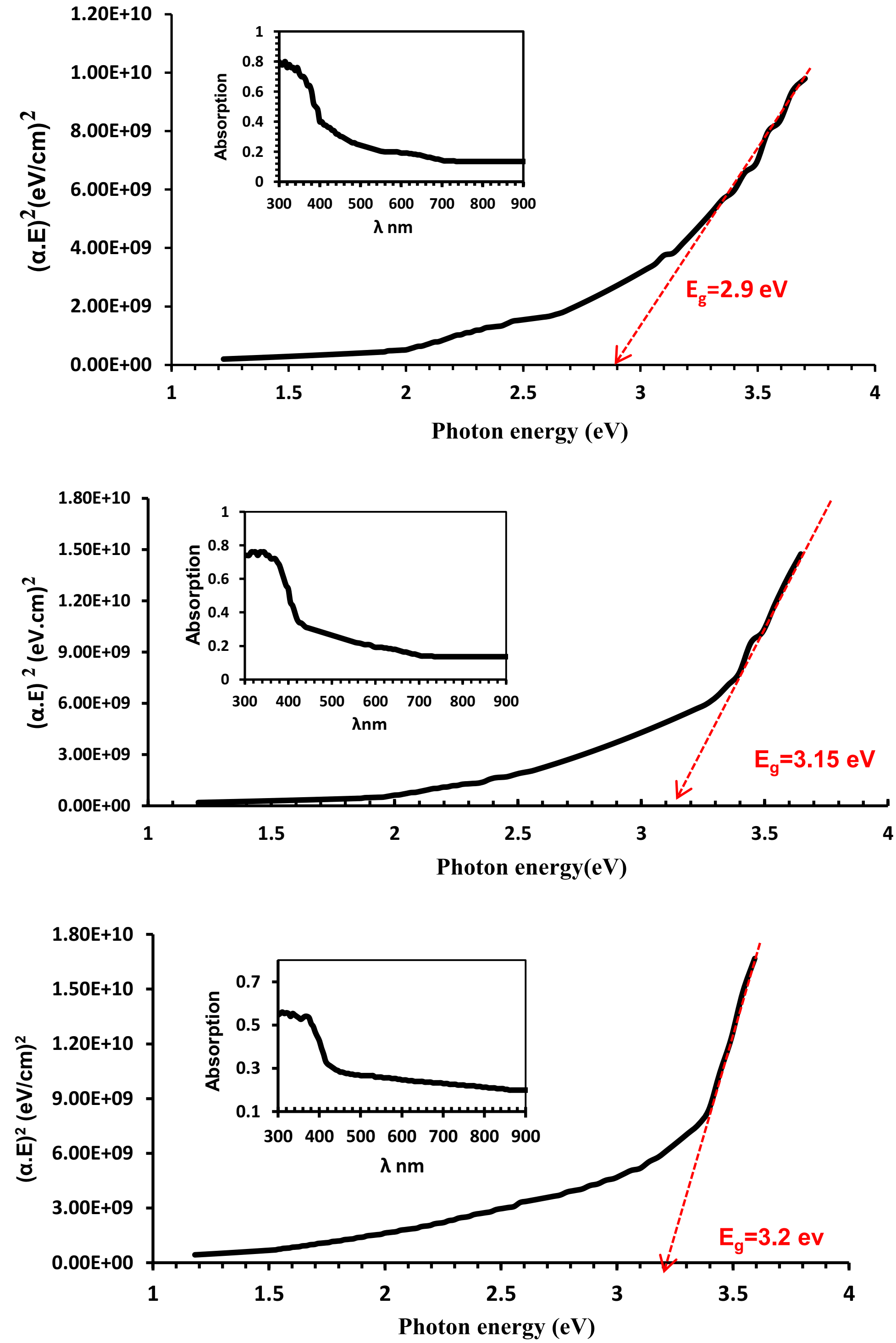

Fig. 3 Variation of $(\alpha E)^2$ with photon energy of Nb_2O_5 film **a** substrate at 45° and 1 cm high, **b** substrate at angle 45° and 3 cm height, **c** substrate at 0° angle

4 Conclusions

Nb_2O_5 nanostructured films were deposited by using a facile and cost-effective hydrothermal method with metal Nb powder and water as the precursors. Films were obtained with different surface morphologies and structural properties depending on the substrate position and deposition angle. Optical data revealed that optical energy gap of the film increased with the height and angle of the substrate. A high-quality spring- and flake-like nanostructure

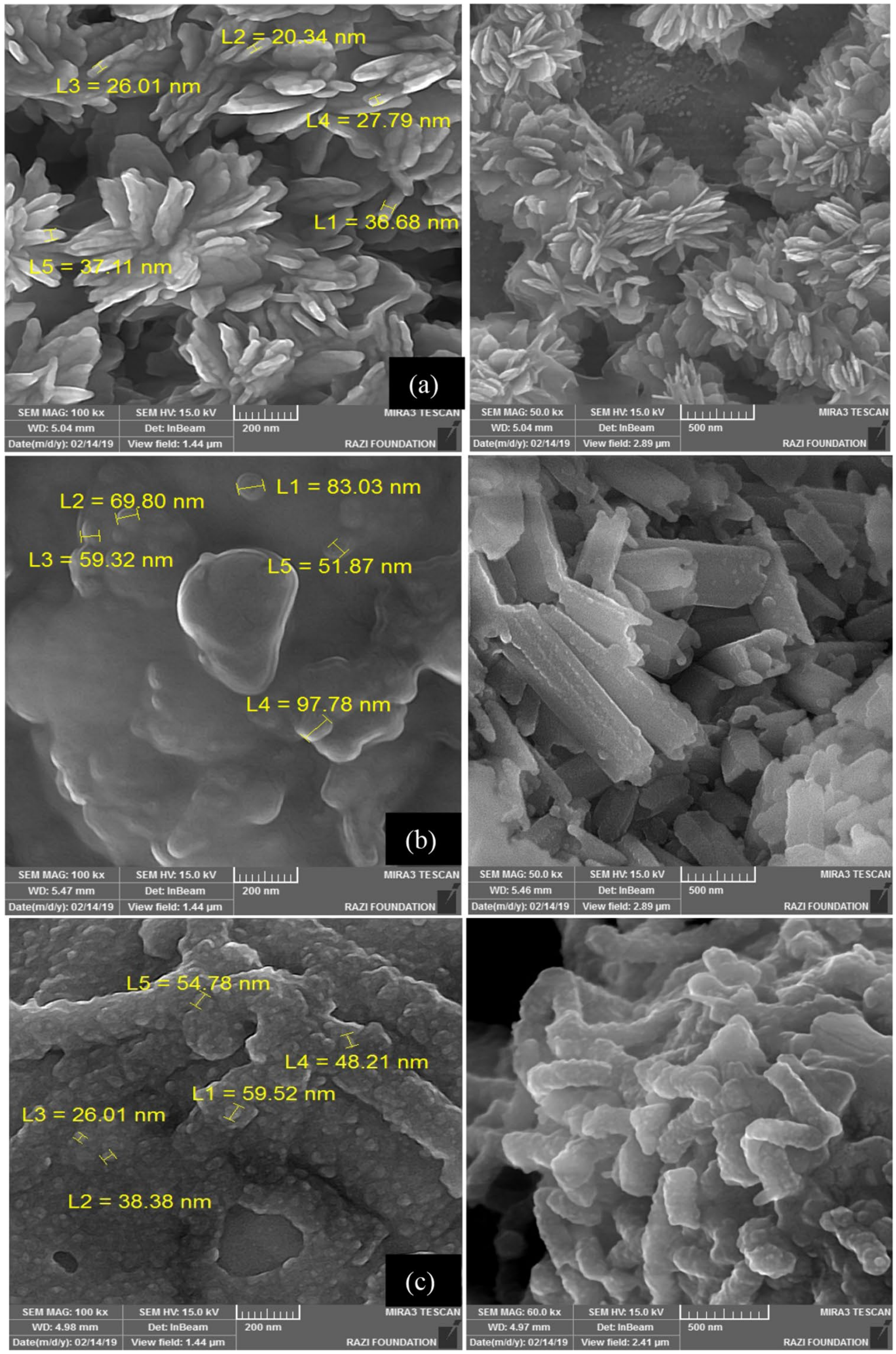

Fig. 4 (Left) SEM images of Nb_2O_5 thin films prepared at three different positions **a** substrate at 45° and 1 cm high, **b** substrate at angle 45° and 3 cm height, **c** substrate at 0° angle (right) magnified SEM images

could be obtained with 87%–99% material stoichiometry using different sample holder designs inside the closed autoclave.

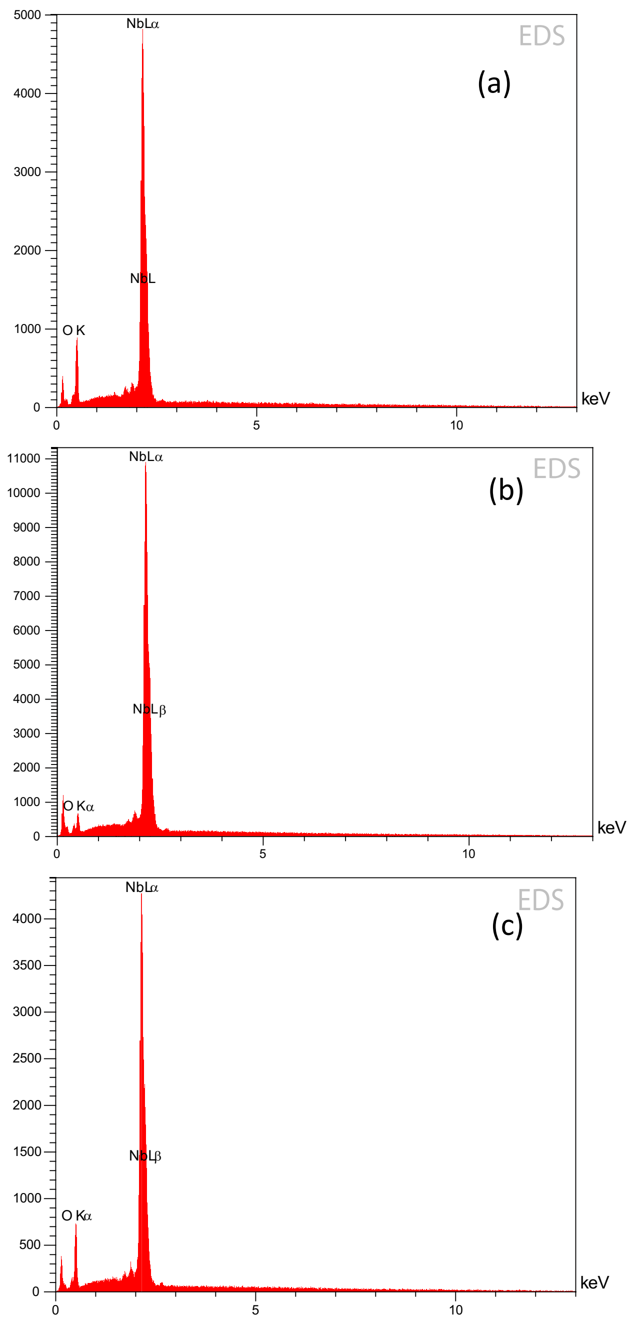

Fig. 5 EDX spectra of Nb_2O_5 sample deposited at **a** substrate at 45° and 1 cm high, **b** substrate at angle 45° and 3 cm height and **c** substrate at 0° angle

Table 2 Mass percentage and stoichiometry of prepared sample at different preparation conditions

Angle of thin film	Nb%	O%	Nb/O
45° with height 1 cm	67.07	32.93	2.04
45° with height 3 cm	85.55	14.45	5.92
Zero angle flat substrate	69.93	30.07	2.32

References

1. K.-N. Chen, C.-M. Hsu, J. Liu, Y.-C. Liou, C.-F. Yang, Investigation of antireflection Nb_2O_5 thin films by the sputtering method under different deposition parameters. Micromachines **7**, 151 (2016)
2. M.A. Fakhri, E.T. Salim, M.H. Wahid, A.W. Abdulwahhab, Z.T. Salim, U. Hashim, Heat treatment assisted-spin coating for $LiNbO_3$ films preparation: their physical properties. J. Phys. Chem. Solids **131**, 180–188 (2019)
3. C.O. Avellaneda, A. Pawlicka, M.A. Aegerter, Two methods of obtaining sol–gel Nb2O5 thin films for electrochromic devices. J. Mater. Sci. **33**, 2181–2185 (1998)
4. S.M. Taleb, M.A. Fakhri, S.A. Adnan, Substrate and annealing temperatures effects on the structural results of $LiNbO_3$ photonic films using PLD method. AIP Conf. Proc. **2213**(1), 020234 (2020)
5. C. Nico, T. Monteiro, M.P.F. Graça, Niobium oxides and niobates physical properties, review and prospects. Prog. Mater Sci. **80**, 1–37 (2016)
6. M.K. Abood, E.T. Salim, J.A. Saimon, Impact of substrate type on the microstructure of H-Nb_2O_5 thin film at room temperature. Int. J. Nanoelectron. Mater. **11**, 55–64 (2018)
7. M.A. Fakhri, A.W. Abdulwahhab, M.A. Dawood, A.I. Sabah, Nano silver oxide based on insulator for optoelectronic device. AIP Conf. Proc. **2213**(1), 020226 (2020)
8. C.C. Lee, C.L. Tien, J.C. Hsu, Internal stress and optical properties of Nb_2O_5 thin films deposited by ion-beam sputtering. Appl. Opt. **41**, 2043–2047 (2002)
9. R. Romero, J.R. Ramos-Barrado, F. Martin, D. Leinen, Nb_2O_5 thin films obtained by chemical spray pyrolysis. Surf. Interface Anal. **36**, 888–891 (2004)
10. S.M. Taleb, M.A. Fakhri, S.A. Adnan, Physical investigations of nanophotonic $LiNbO_3$ films for photonic applications. J. Ovonic Res. **15**(4), 261–269 (2019)
11. D. Rosenfeld, P.E. Schmid, S. Szeles, F. Levy, V. Demarne, A. Grisel, Sens. Actuators B **37**, 83–89 (1996)
12 S. Venkataraj, R. Drese, Ch Liesch, O. Kappertz, R. Jayavel, M. Wuttig, J. Appl. Phys. **91**, 4863 (2002)
13. E.T. Salim, R.A. Ismail, H.T. Halbos, Growth of Nb_2O_5 film using hydrothermal method: effect of Nb concentration on physical properties. Mater. Res. Express **6**, 116429 (2019)
14. Y.D. Wang, L.F. Yang, Z.L. Zhou, Y.F. Li, X.H. Wu, Effects of calcining temperature on lattice constants and gas-sensing properties of Nb_2O_5. Mater. Lett. **49**, 277–281 (2001)
15 R.A. Rani, A.S. Zoolfakar, J. Subbiah, J.Z. Ou, K. Kalantarzadeh, Highly ordered anodized Nb2O5 nanochannels for dye-sensitized solar cells. Electrochem. Commun. **40**, 20–24 (2014)
16. S.M. Taleb, M.A. Fakhri, S.A. Adnanm, Optical investigations of nanophotonic $LiNbO_3$ films deposited by pulsed laser deposition method. Defect Diffus. Forum **398**, 16–22 (2020)
17. C. Nico, T. Monteiro, M.P.F. Graça, Niobium oxides and niobates physical properties: review and prospects. Prog. Mater. Sci. **80**, 1–37 (2016)
18. I. Zhitomirsky, Electrolytic deposition of niobium oxide films. Mater. Lett. **35**, 188–193 (1998)
19. K. Kamada, M. Mukai, Y. Matsumoto, Anodic dissolution of tantalum and niobium in acetone solvent with halogen additives for electrochemical synthesis of Ta_2O_5 and Nb_2O_5 thin films. Electrochim. Acta. **49**, 321–327 (2004)
20. T.-Y. Cho, K.-W. Ko, S.-G. Yoon, Efficiency enhancement of flexible dye-sensitized solar cell with sol–gel formed Nb_2O_5 blocking layer. Curr. Appl. Phys. **13**, 1391–1396 (2013)
21. A. Verma, P.K. Singh, Sol-gel derived nanostructured niobium pentoxide thin films for electrochromic applications. Indian J. Chem. Sect. **52**(5), 593–598 (2013)

22. E. Çetinörgü-Goldenberg, J.-E. Klemberg-Sapieha, L. Martinu, Effect of postdeposition annealing on the structure, composition, and the mechanical and optical characteristics of niobium and tantalum oxide films. Appl. Opt. **51**, 6498–6507 (2012)
23 J.M. Weisse, C.H. Lee, D.R. Kim, X. Zheng, Fabrication of flexible and vertical silicon nanowire electronics. Nano Lett. **12**, 3339–3343 (2012)
24. M.A. Fakhri, N.H. Numan, Q.Q. Mohammed, M.S. Abdulla, O.S. Hassan, S.A. Abduljabar, A.A. Ahmed, Responsivity and response time of nano silver oxide on silicon heterojunction detector. Int. J. Nanoelectron. Mater. **11**(Special Issue BOND21), 109–114 (2018)
25. A. Dhar, T.L. Alford, Optimization of Nb_2O_5/ Ag/Nb_2O_5 multilayers as transparent composite electrode on flexiblesubstrate with high figure of merit. J. Appl. Phys. **112**, 103113 (2012)
26 R. Ghosh, M.K. Brennaman, T. Uher, M.R. Ok, E.T. Samulski, L.E. McNeil, T.J. Meyer, R. Lopez, Nanoforest Nb2O5 photoanodes for dye-sensitized solar cells by pulsed laser deposition. ACS Appl. Mater. Interfaces **3**, 3929–3035 (2011)
27. S. Hyunjun, C. Dooho, L. Dongsoo, S. Seo, M. Lee, I. Yoo, H. Hwang, Resistance-switching characteristics of polycrystalline $Nb_2O_5$for nonvolatile memory application. IEEE Electron Device Lett. **26**, 292–294 (2005)
28. M.A. Fakhri, E.T. Salim, M.H.A. Wahid, Z.T. Salim, U. Hashim, A novel parameter effects on optical properties of the $LiNbO_3$ films using sol-gel method. AIP Conf. Proc. **2213**(1), 020242 (2020)
29. H. Asady, E.T. Salim, R.A. Ismail, Some critical issues on the structural properties of Nb_2O_5 nanostructure film deposited by hydrothermal technique. AIP Conf. Proc. **2213**(1), 020183 (2020)
30. C.-C. Lee, C.-L. Tien, J.-C. Hsu, Internal stress and optical properties of Nb_2O_5 thin filmsdeposited by ion-beam sputtering. Appl. Opt. **41**, 2043–2047 (2002)
31. T. Murayama, J. Chen, J. Hirata, K. Matsumoto, W. Ueda, Hydrothermal synthesis of octahedra-based layered niobium oxide and its catalytic activity as a solid acid. Catal. Sci. Technol. **4**, 4250–4257 (2014)
32. Y. Zhao, C. Eley, J. Hu, J.S. Foord, L. Ye, H. He, S.C.E. Tsang, Shape-dependent acidityand photocatalytic activity of Nb_2O_5 nanocrystals with an active TT (001) surface. Angew. Chem. Int. Ed. **51**, 3846–3849 (2012)
33. K. Saito, A. Kudoa, Diameter-dependent photocatalytic performance of niobium pentoxidenanowires. Dalton Trans. **42**, 6867–6872 (2013)
34. G. Demazeau, Solvothermal and hydrothermal processes: the main physico-chemical factors involved and new trends. Res. Chem. Intermed. **37**, 107–123 (2011)
35. G. Yang, S.J. Park, Conventional and microwave hydrothermal synthesis and application of functional materials: a review. Materials **12**, 1177 (2019)
36. V. Galstyan, E. Comini, G. Faglia, G. Sberveglieri, Synthesis of self-ordered and well aligned Nb_2O_5 nanotubes. Cryst. Eng. Commun. **16**, 10273–10279 (2014)
37. X. Liu, R. Yuan, Y. Liu, S. Zhu, J. Lin, X. Chen, Niobium pentoxide nanotube powder for efficient dye-sensitized solar cells. New J. Chem. **40**, 6276–6280 (2016)
38. J. Hu, L. Li, H. Lin, P. Zhang, W. Zhou, Z. Ma, Flexible integrated photonics: where materials, mechanics and optics meet. Opt. Mater. Express **3**, 1313–1331 (2013)
39. M. Wei, Z.-M. Qi, M. Ichihara, H. Zhou, Synthesis of single-crystal niobium pentoxidenanobelts. Acta Mater. **56**, 2488–2494 (2008)
40. P. Wen, L. Ai, T. Liu, D. Hu, F. Yao, Hydrothermal topological synthesis and photocatalyst performance of orthorhombic Nb_2O_5 rectangle nanosheet crystals with dominantly exposed (010) facet. Mater. Design **117**, 346–352 (2017)
41. H. Luo, M. Wei, K. Wei, nanosheets and its electrochemical measurements. Mater. Chem. Phys. **120**, 6–9 (2010)
42. S. Li, R. Nechache, I.A.V. Davalos, G. Goupil, L. Nikolova, M. Nicklaus, J. Laverdiere, A. Ruediger, F. Rosei, nanoplates. J. Am. Ceram. Soc. **96**(10), 3155–3162 (2013)
43. K. Byrappa, M. Yoshimura, *Handbook of hydrothermal technology*, 2nd edn. (William Andrew, 2013) **(Hardcover ISBN:9780123750907, eBook ISBN:9781437778366)**
44. H. Bai, F. Guo, B. Zhang, One-step synthesis of high pure CdS nanofilms via hydrothermal method. J. Mater. Sci. Mater. Electron. **29**, 9193–9199 (2018)
45. M.A. Fakhri, S.F.H. Alhasan, N.H. Numan, J.M. Taha, F.G. Khalid, Effects of laser wavelength on some of physical properties of Al_2O_3 nano films for optoelectronic device. AIP Conf. Proc. **2213**(1), 020227 (2020)
46 F.N. Meng, Y. Wang, P. Gao, G.L. Zhang, L.Q. Wang, G.R. Chen, S.Q. Yang, D. Bao, Macroporous ZnO nanofilms and its electrochemical hydrogen storage ability. Adv. Mater. Res. **457–458**, 815–818 (2012)
47. A.S. Ibraheam, J.M. Rzaij, Makram A Fakhri, AW Abdulwahhab, Structural, optical and electrical investigations of Al:ZnO nanostructures as UV photodetector synthesized by spray pyrolysis technique. Mater. Res. Express **6**(5), 055916 (2019)
48. D.P. VolantI, D. Keyson, L.S. Cavalcante, A.Z. Simões, M.R. Joya, E. Longo, J.A. Varela, P.S. Pizani, A.G. Souza, Synthesis and characterization of CuO flower-nanostructure processing by a domestic hydrothermal microwave. J. Alloy. Compd. **459**(1–2), 537–542 (2008). https://doi.org/10.1016/j.jallcom.2007.05.023
49 D.V. Bavykin, V.N. Parmon, A.A. Lapkin, F.C. Walsh, The effect of hydrothermal conditions on the mesoporous structure of TiO_2 nanotubes. J. Mater. Chem. **14**, 3370–3377 (2004)
50. C. Wang, G. Zhang, S. Fan, Y. Li, Hydrothermal synthesis of PbSe, PbTe semiconductor nanocrystals. J. Phys. Chem. Solids **62**(11), 1957–1960 (2001)
51. K. Skrodczky, M. Antunes, X. Han, S. Santangelo, G. Scholz, A.A. Valente, N. Pinna, P.A. Russo, Niobium pentoxide nanomaterials with distorted structures as efficient acid catalysts. Commun. Chem. **2**, 129 (2019)
52. K. Kaempf, Grösse und ursache der doppelbrechung in kundtschenspiegeln und erzeugung von doppelbrechung in metallspiegelndurchzug. Ann. Phys. **321**, 308–333 (1905)
53. O.A. Abdulrazzaq, E.T. Saleem, Inexpensive near-IR photodetector. Turk. J. Phys. **30**, 35–39 (2006)
54. A. Barranco, A. Borras, R. Agustin, G.A. Palmero, Perspectives on oblique angle deposition of thin films: from fundamentals to devices. Prog. Mater Sci. **76**, 59–153 (2016)
55. F. Hattab, M. Fakhry, Optical and structure properties for nano titanium oxide thin film prepared by PLD. In *2012 First National Conference for Engineering Sciences (FNCES 2012)*. https://doi.org/10.1109/NCES.2012.6740474
56. J. He, Y. Hu, Z. Wang, W. Lu, S. Yang, G. Wu, Y. Wang, S. Wang, H. Gu, J. Wang, Hydrothermal growth and optical properties of Nb2O5 nanorod arrays. J. Mater. Chem. C **2**, 8185–8190 (2014)
57 H. Luo, M. Wei, K. Wei, Synthesis of Nb2O5 nanorods by a soft chemical process. J. Nanomater. (2009). https://doi.org/10.1155/2009/758353
58 M.A. Muhsien, E.T. Salim, I.R. Agool, Preparation and characterization of (Au/n-SnO2/SiO2/Si/Al) MIS device for optoelectronic application. Int. J. Opt. **2013**, 9 (2013). https://doi.org/10.1155/2013/756402
59 E.T. Salim, M.A. Fakhri, R.A. Ismail, A.W. Abdulwahhab, Z.T. Salim, M.A. Munshid, U. Hashim, Effect of light induced heat treatment on the structural and morphological properties of $LiNbO_3$ thin films. Superlattices Microstruct. **128**, 67–75 (2019)

60 R. Ismail, Improved characteristics of sprayed CdO films by rapid thermal annealing. J. Mater. Sci. Mater. Electron. **20**, 1219–1224 (2009)
61 R.A. Ismail, O.A. Abdulrazaq, K. Yahya, Preparation and characterization of In_2O_3 thin films for optoelectronic applications. Surf. Rev. Lett. **12**, 515–518 (2005)
62. M.A. Muhsien, E.T. Salim, Y. Al-Douri, A.F. Sale, I.R. Agool, Synthesis of SnO2 nanostructures employing Nd:YAG laser. Appl. Phys. A Mater. Sci. Process. **120**(2), 725–730 (2015)
63. N. Ghobadi, Band gap determination using absorption spectrum fitting procedure. Int. Nano Lett. **3**, 2–5 (2013)
64. R. Ismail, K. Khashan, R. Mahdi, Characterization of high photosensitivity nanostructured 4H-SiC/p-Si heterostructure prepared by laser ablation of silicon in ethanol. Mater. Sci. Semicond. Process. **68**, 252–261 (2017)
65 M.A. Fakhri, E.T. Salim, A.W. Abdulwahhab, U. Hashim, M.A. Minshid, Z.T. Salim, The effect of annealing temperature on optical and Photolumence Properties of $LiNbO_3$. Surf. Rev. Lett. **26**(10), 1950068 (2019)
66 E.T. Salim, Surface morphology and X-ray diffraction analysis for silicon nanocrystal-based heterostructures. Surf. Rev. Lett. **20**(05), 1350046 (2013)
67. R.A. Ismail, A.M. Alwan, A.S. Ahmed, Preparation and characteristics study of nano-porous silicon UV photodetector. Appl. Nanosci. **7**, 9–15 (2017)
68. B. Fan, H.K.M. Vithana, J.C. Kralik, S.M. Faris, Optical circular dichroism of vacuum-deposited film stacks. Opt. Commun. **147**, 265–268 (1998)
69. M.A.M. Hassan, M.F.H. Al-Kadhemy, E.T. Salem, Effect irradiation time of Gamma ray on MSISM ($Au/SnO_2/SiO_2/Si/Al$) devices using theoretical modeling. Int. J. Nanoelectron. Mater. **8**(2), 69–82 (2014)
70. R. Alvarez, C. Lopez-Santos, J. Parra-Barranco, V. Rico, A. Barranco, J. Cotrino, A.R. Gonzalez-Elipe, A. Palmero, Nanocolumnar growth of thin films deposited at oblique angles: Beyond the tangentrule. J. Vacuum Sci. Technol. B **32**, 041802 (2014). https://doi.org/10.1116/1.4882877